Bulletin of Geophysics and Oceanography Vol. 67, n. 1, pp. 159-172; March 2026
DOI 10.4430/bgo00520

Optimised SARIMA models to forecast changes in ocean acidification and atmospheric CO_2

N. Rodríguez

Villa del Rosario, Colombia

(Received: 8 March 2025; accepted: 27 November 2025; published online: 18 March 2026)

ABSTRACT Regression methods are widely used to model, smooth, and forecast datasets, whether in time series, scattered data, or logistic variables. Besides, linear regression is often preferred due to its simplicity and efficiency in identifying trends. However, many real-world phenomena, such as climate change, economic fluctuations, gambling, and biological processes, exhibit nonlinear behaviours that require more advanced regression techniques. For this reason, some studies include polynomial, exponential, and dynamic approaches derived from linear models. This study focuses on ocean acidification and carbon dioxide (CO_2) emissions, two interconnected factors influencing climate change and marine ecosystems. Both datasets are structured as time series, where ocean acidification is measured in seawater pH levels, and CO_2 emissions are recorded in parts per million. To perform a deep data analysis, this paper sets up a particular seasonal autoregressive integrated moving average model for prediction in order to process volatile time series with complex trends, providing, thus, a scalable and effective long-term forecasting technique.

Key words: SARIMA model, forecasting methods, climate change, carbon dioxide emissions, ocean acidification.

1. Introduction

Since the mid-20th century, the continuous increase in atmospheric carbon dioxide (CO_2) has led to measurable chemical changes in seawater, notably a persistent decrease in pH known as ocean acidification. The Keeling curve (Keeling *et al.*, 1976) established the long-term record of atmospheric CO_2 at Mauna Loa Observatory, revealing the direct impact of anthropogenic emissions. Subsequent studies demonstrated that approximately 30–40% of this CO_2 is absorbed by the ocean, forming carbonic acid and reducing the availability of carbonate ions necessary for calcifying organisms (Zeebe *et al.*, 2008).

Ocean acidification weakens marine ecosystems and threatens food security, prompting the inclusion of both atmospheric CO_2 rise and ocean pH decline among the nine planetary boundaries (Rockstrm *et al.*, 2009). Therefore, the modelling of future pH evolution is vital to estimate when critical thresholds, such as pH 7.0, may be reached.

Previous approaches have mainly relied on process-based models, such as those by Caldeira Wickett (2005), which simulate ocean circulation and carbonate chemistry under emission scenarios. Although physically robust, these models depend on complex boundary conditions and assumptions. In contrast, statistical time-series models can capture empirical patterns directly from observations and provide practical forecasting when physical parameters are uncertain.

This study applies optimised models based on seasonal autoregressive integrated moving average (SARIMA) to the global ocean pH record (1985–2022) to evaluate their predictive capability and contrast them with traditional linear models. Atmospheric CO_2 is considered as an exogenous or contextual variable that influences ocean pH, rather than an independent forecasting target. The ultimate goal is to assess whether autoregressive models can reproduce observed variability and produce scenario-based projections consistent with physical expectations.

2. Research summary

2.1. Hydrogen potential

In ocean systems, the average surface pH currently measures approximately 8.04, having declined from about 8.11 in 1985 to 8.04 in 2024, according to global observational datasets (Copernicus Marine Service, 2022; NOAA, 2025). This corresponds to an average change rate of approximately 0.0017 pH units per year, equivalent to an increase of about 30% in hydrogen ion concentration since pre-industrial times (Sutton *et al.*, 2022; EEA, 2024). Although ocean pH remains slightly basic, this gradual acidification represents a significant shift in marine chemistry, altering carbonate equilibrium and threatening calcifying organisms and ecosystem stability.

2.2. Regression methods

Regression analyses provide a basic framework for identifying trends in environmental data. Linear regression models, including ordinary least squares (OLS) and least absolute deviation, are frequently used due to their computational simplicity and interpretability. However, these methods assume linearity, independence, and constant variance, assumptions rarely satisfied in geophysical time series. Ocean pH exhibits autocorrelation and irregular seasonal oscillations that cannot be adequately captured by a fixed-slope model.

Consequently, while linear models can describe the general downward trend in pH, they fail to reproduce short-term fluctuations or nonlinear interactions between physical and chemical

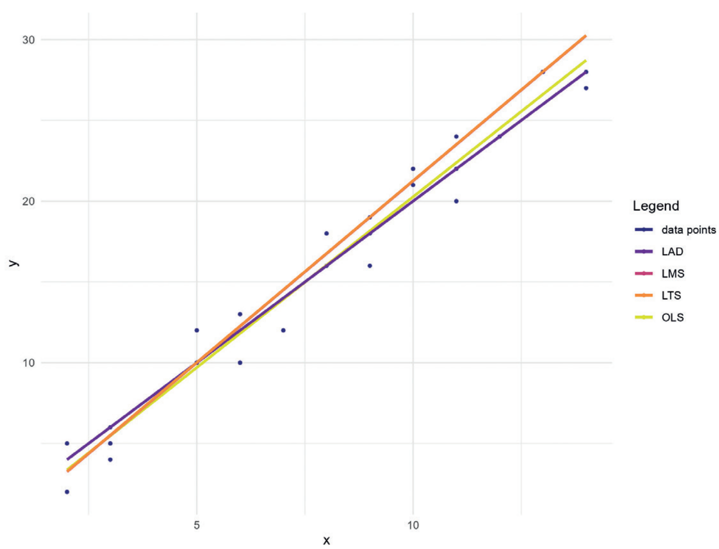

Fig. 1 - Sample of linear regression models with a small set of random points represented by a straight line.

drivers. These limitations motivate the adoption of autoregressive approaches capable of controlling non-stationary and periodic behaviour, as discussed in the following section.

The sample in Fig. 1 highlights how the OLS classical method significantly changes its slope and interception point, and how some methods, like the least square method, are completely inaccurate, because they remain ineffective in the presence of outliers. Therefore, in order to choose the best model, it is necessary to compare error metrics like the mean absolute error (*MAE*) or median absolute deviation, as the best model expresses the lowest values of such metrics (Dodge, 2008).

2.3. Non-stationarity and seasonality

Statistical metrics such as arithmetic mean, variance, and standard deviation enable to extract useful information from any database; for instance, in the case of scatter datasets, the arithmetic mean is used to report central tendencies despite its lack of robustness dealing with outliers, while the variance and standard deviation reflect the degree of data dispersion, being the former one usually preferred although the latter is expressed in the same units as the variable (Villavicencio, 2018).

In the case of time series, statistical metrics operate in several different ways. The total mean or average is used to divide the time series in halves. The comparison of the means of such resultant subsets defines the stationarity of the series. In addition, the statistical measures can be used as moving metrics to study the variability of the time series within specific time segments (rolling standard deviation) or to add another stationarity test through graphic analyses (rolling mean); thus, if one of such metrics changes considerably over time, the series exhibits low or null stationarity, which facilitates the finding of the suitable prediction model, as some of the forecasting methods work better depending on the stationarity and seasonality of the time series to be manipulated (Box *et al.*, 2016).

2.4. Predictive model

The autoregressive integrated moving average (ARIMA) model (Box and Jenkins, 1970) is widely used for short- and medium-term forecasting in non-stationary time series. However, when seasonal fluctuations are present, an extended version, known as the SARIMA model, is more appropriate. The SARIMA model introduces seasonal autoregressive and moving-average components defined by period s and parameters (P, D, Q), leading to the general form:

$$SARIMA\ (p, d, q)\ (P, D, Q)\ [S] \qquad (1)$$

where p is the order of the autoregressive component, which represents the relationship between an observation and a number of previous observations (lags). Parameter d is the degree of non-seasonal differentiation (integration) applied to the time series to make it stationary. As of q, it is the order of the moving average component, which captures the relationship between an observation and the forecast errors of a number of previous observations. P is the order of the seasonal autoregressive component, D is the degree of seasonal differentiation required to make the series stationary in its seasonal cycle, and Q is the order of the seasonal moving average component; finally, s is the number of observations in each seasonal cycle. For example, s = 12 for monthly data with an annual cycle. This structure enables the model to capture both long-term trends and recurring oscillations that characterise climate-related datasets.

In this work, the SARIMA framework was selected to model monthly ocean pH observations (1985–2022). Since ocean pH exhibits irregular cycles influenced by atmospheric CO_2, a drift term was incorporated to represent the persistent long-term decline. The Auto.arima() function from the *forecast* package in R (Hyndman and Khandakar, 2008) was used to automatically identify the optimal model structure based on the minimisation of the Bayesian information criterion (*BIC*). Only seasonal structures with a 12-month frequency were considered.

To assess the model's predictive capability, the dataset was divided into a training set (1985–2020) and a testing set (2021–2022). The training data were used for model fitting and the last 24 monthly observations were reserved for out-of-sample validation. Model performance was evaluated through the root-mean-square error (*RMSE*) and *MAE* between the predicted and actual pH values in the test set.

Finally, once the optimal model was confirmed, long-term forecasts were generated under two scenarios: 1) baseline (empirical extrapolation), assuming continuation of historical patterns; 2) scenario-conditioned, using seasonal-trend decomposition (STL) using locally estimated scatterplot smoothing (LOESS) and ARIMA models to obtain approximations to long-term values.

2.5. Seasonal-trend decomposition using locally estimated scatterplot smoothing

STL is a robust, nonparametric approach for decomposing time series into three additive components: trend, seasonal, and remainder (Cleveland *et al.*, 1990). Unlike traditional decomposition methods that assume a fixed seasonal structure, STL employs locally weighted regression methods (like LOESS), to adaptively estimate the seasonal pattern and long-term trend. This flexibility makes STL highly effective in dealing with environmental time series where seasonal strength and noise can vary over time (Hyndman and Athanasopoulos, 2021).

By combining STL with ARIMA modelling of the residual component, the model integrates the interpretability of decomposition with the predictive strength of stochastic modelling. This hybrid approach enables each component of the series to be separately modelled: the trend captures the long-term direction, the seasonal component captures recurring oscillations, and ARIMA captures the short-term autocorrelations and irregular variations (De Livera *et al.*, 2011).

Empirical studies show that STL + ARIMA models often outperform standalone SARIMA for medium- and long-term forecasts, particularly when the underlying process exhibits evolving seasonality or nonlinear trends (Hyndman *et al.*, 2015). This hybridisation improves model stability and reduces the propagation of forecast error compared to pure autoregressive approaches, making it particularly suitable for climate and oceanographic variables such as pH, temperature, or CO_2 concentration.

2.6. Case studies

2.6.1. Data description and preparation

The datasets analysed in this study comprise monthly mean records of ocean pH and atmospheric CO_2. Ocean pH data were obtained from the Copernicus Marine Environment Monitoring Service, covering the period from January 1985 to December 2022, and represent global surface-ocean means derived from *in-situ* and model-based reanalysis products. Atmospheric CO_2 data, expressed in parts per million (ppm), were retrieved from the Mauna Loa Observatory (NOAA, 2024). Both datasets were aligned by timestamp to ensure temporal consistency and, then, only months available in both records were retained. The original pH data contained several missing monthly values, mostly before 1990, which were treated through linear interpolation to preserve the required monthly frequency. To minimise the influence of local anomalies or observational noise, both series were standardised (zero mean, unit variance) prior to model fitting.

Both ocean pH and atmospheric CO_2 time series (Figs. 2 and 3, respectively) exhibit well-documented long-term trends and weak seasonal components driven by climatic and biogeochemical variability. The decline in surface-ocean pH is recognised as non-stationary due to the persistent accumulation of atmospheric CO_2 and its dissolution in seawater (Caldeira and Wickett, 2005; Doney *et al.*, 2009; Sutton *et al.*, 2022).

As such, the pH series was differenced to achieve stationarity before parameter estimation in the SARIMA framework. A 12-month periodicity was assumed to capture the seasonal cycle, consistent with the monthly sampling frequency. This preprocessing ensured that residuals exhibited no systematic trend or autocorrelation, satisfying the model assumptions of weak stationarity.

The final dataset consisted of 456 monthly observations from 1985 to 2022. For model validation, the data were divided into two subsets:

1) training set: January 1985 – December 2020 (90% of the data), used for model estimation;
2) testing set: January 2021 – December 2022 (24 samples), reserved for out-of-sample evaluation.

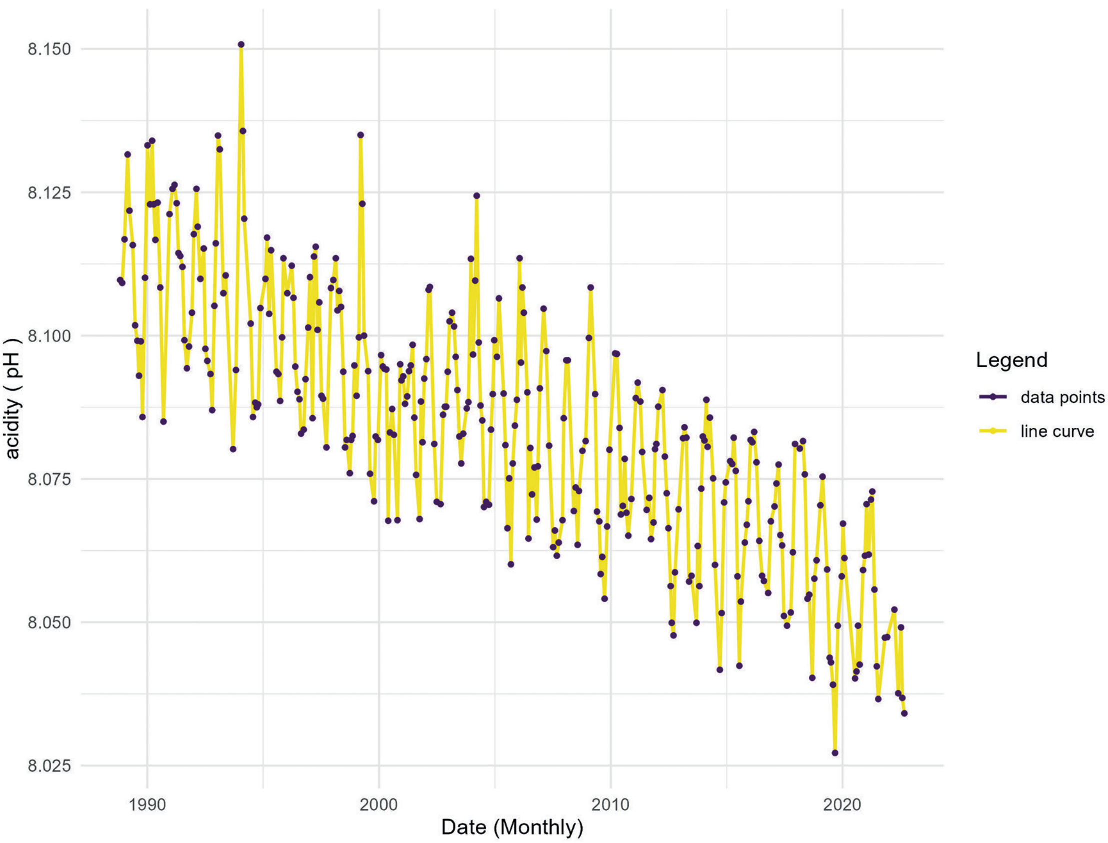

Fig. 2 - Ocean pH dataset with the original time series of ocean acidification extracted from the Copernicus Marine Service website.

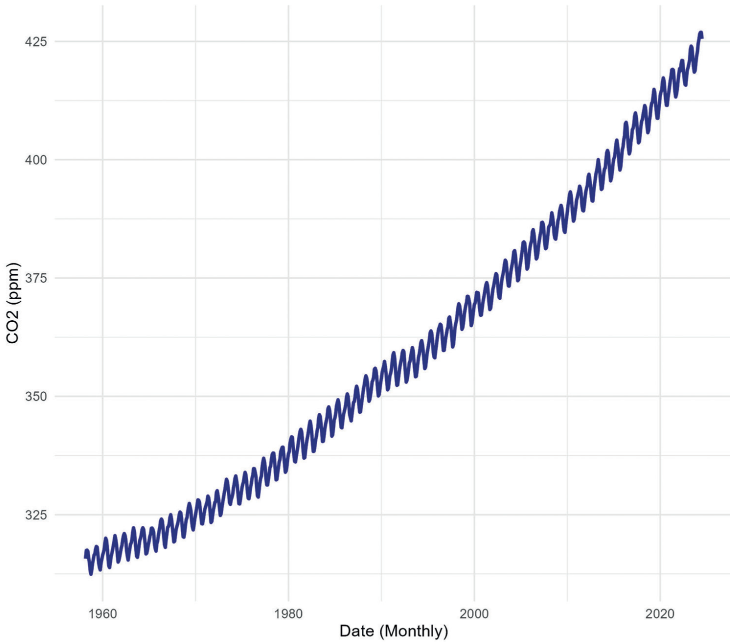

Fig. 3 - Carbon dioxide (CO_2) emission dataset with the original time series of the atmospheric CO_2 extracted from the NASA website.

The sampling frequency of 12 observations per year was maintained for both the regression and ARIMA models, enabling direct comparison of their outputs. This division ensured that prediction accuracy was evaluated on unseen data, avoiding overfitting and providing a fair assessment of the generalisation capability of each model.

2.6.2. Finding the optimum parameters for the models

Parameter selection for the SARIMA models followed a two-step approach. First, a manual exploratory search was carried out to understand the sensitivity of model performance to changes in the autoregressive (p) and moving average (q) terms. This initial grid search explored combinations of $p, q \in [0, 5]$ and differencing orders d = 0.1, along with seasonal components (P,D,Q) for a fixed period of 12 months, corresponding to the monthly sampling frequency.

In the second step, the Auto.arima() function from the *forecast* package in R (Hyndman Khandakar, 2008) was applied to confirm the optimal configuration using the Akaike information criterion corrected (*AICc*). This automated selection corroborated the best-performing model previously identified during the manual exploration, thus combining interpretability and objective statistical optimisation. Model performance was evaluated according to three information criteria: the Akaike information criterion (*AIC*), *BIC*, and residual standard error (*SE*). *AIC* and *BIC* are defined respectively as:

$$AIC = 2k - 2ln(L), \quad BIC = kln(n) - 2ln(L) \tag{2}$$

where k represents the number of estimated parameters, n the sample size, and L the model likelihood.

While lower values of *AIC* and *BIC* indicate a more parsimonious fit, the *SE* measures the dispersion of residuals.

3. Experiments

3.1. Linear regression

As a first approach, the linear model consolidates all the information as a fixed slope and, therefore, the curve in Fig. 4 is obtained for the pH dataset.

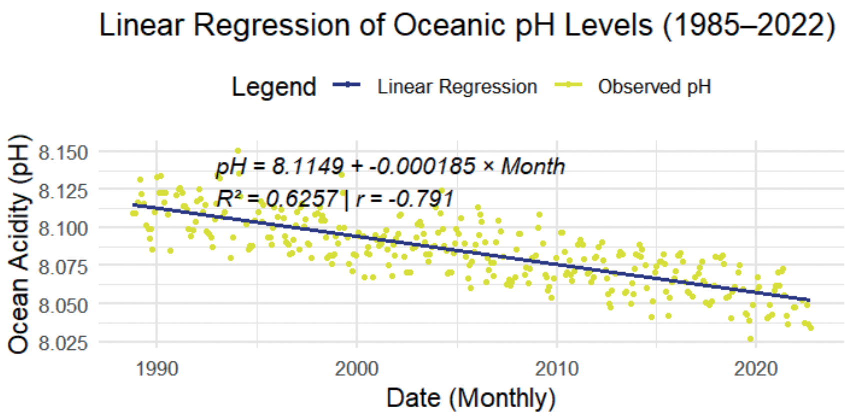

Fig. 4 - Linear model for ocean pH with the scatterplot of the original data points with the linear approach and its respective mathematical expression.

This model considers the months as numerical amounts and, thereby, any positive integer *x* introduced calculates the ocean pH for *x* months as of October 1985. As might be expected, this model needs a considerable amount of data to deal with possible outliers and low dispersion to provide a decent forecast in cases of simple predictions without crucial purposes, namely, it provides a poor but basic idea of when the ocean pH could be closer to seven.

The same method is applied to the CO_2 dataset, generating the plot in Fig. 5. In this case, the model has a steeper slope in comparison to the one displayed in Fig. 4; and, in fact, the linear model is no longer suitable, as the dataset reflects curves as a quadratic or even exponential trend. However, analogously to the case of the ocean-pH dataset, the equation enables performing

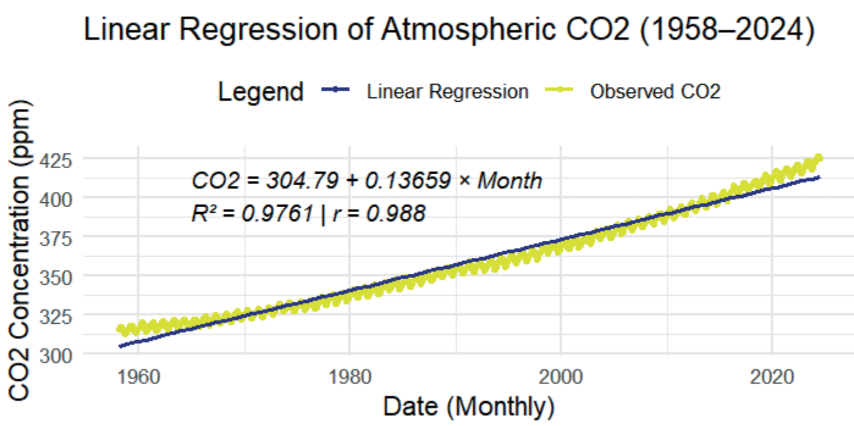

Fig. 5 - Linear model for CO_2 emissions from 1958 to 2024 with the straight-line curve taking into account the whole dataset of atmospheric CO_2 and displaying the respective equation.

basic forecasts (in this case as of 2024). Moreover, this linear model highlights how the length of the time series modifies the slope. Unlike the ocean-pH series, the CO_2 series adds almost 30 years to the timeline (Fig. 6).

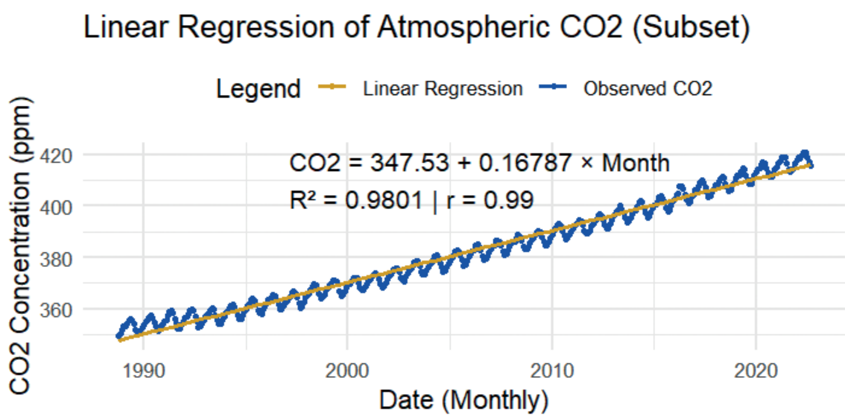

Fig. 6 - Linear model for CO_2 emissions from 1988 to 2022 with the straight-line curve taking into account only the 1988–2022 atmospheric CO_2 segment and its new mathematical expression.

3.2. Forecasting models

As previously mentioned in Section 2.4, an ARIMA model will be used to perform short-term predictions. Nonetheless, its input parameters should be adjusted according to the specific objectives, as the choice of ARIMA methods depends on the nature of the time series as, for example, non-seasonal series could require a drift or deterministic component, and every change on the *p*, *q*, and *d* parameters would, then, significantly affect the possible next fluctuations. Some authors apply trial and error, and after simulating several parameter combinations, the best model will be the one with the lowest *BIC* and *SE* values. Based on this, in this paper, some models are applied before adjusting an optimal version for each time series considered.

3.2.1. SARIMA model for ocean pH series

Performing trials for every *p*, *q*, and *d* parameter combination and including seasonal components to build an optimal model would be an exhausting job, even for computers. For this reason, only a selection of attempts is registered to emphasise the application of the criteria previously mentioned. The simulations begin with the ocean pH dataset, considering seasonal components, and a drift owing to the trend component.

Table 1 - Different ARIMA models for forecasting the ocean pH dataset.

p	*d*	*q*	*BIC*	*AIC*	Regression *SE*
2	1	0	-1952.073	-1967.257	0.01209
1	1	0	-1957.515	-1968.903	0.01208
1	2	1	-1944.741	-1956.120	0.01210
3	2	1	-1940.910	-1959.875	0.01199
2	3	3	-1911.567	-1934.307	0.01211
3	**1**	**2**	**-2063.361**	**-2089.933**	**0.00994**

Every model fitted via trial and error could meet as optimal model as the standard error and at least BIC are reduced. Nowadays there are methods to find the optimal ARIMA approach for time series like those studied in this paper. Certainly, a variety of tests are included to minimise the criteria displayed in Table 1 and other criteria (e.g. *AICc* or the Hannan-Quinn Information Criterion), and to find optimal order parameters, such as current algorithms based on differencing tests like Kwiatkowski–Phillips–Schmidt–Shin, and Augmented Dickey–Fuller (Smith, 2023). These empirical models simply exhibit a basic orientation to the optimal combination of values. By considering seasonal components *P*, *D*, and *Q*, and period *s*, month-on-month-seasonal *p*, *d*, and *q* values could be modified, and, therefore, the optimal SARIMA model would comply with the description in Table 2.

Table 2 - Optimal SARIMA model for forecasting the ocean pH dataset.

Optimal data								
p	**d**	**q**	**P**	**D**	**Q**	***BIC***	***AIC***	**Regression *SE***
2	1	2	0	0	1	-1853.35	-1879.18	0.00994

This latter model, which clearly shows lower criterion values, is able to test the final 10% of the data.

In Fig. 7, the performance of the SARIMA(1,1,1)(2,1,1)[12] model and the observed ocean pH values, during the independent test period (2021—2022), are compared. The model reproduces both the gradual long-term decline and the weak seasonal oscillations evident in the series. Predicted values (blue dashed line) closely follow the measured data (red line) and remain within the 95% confidence interval, indicating that the uncertainty bounds adequately capture the variability of the observations.

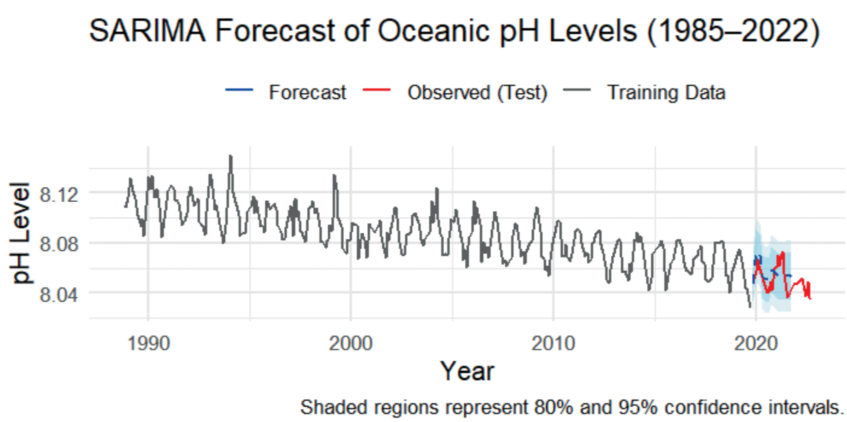

Fig. 7 - Output of the optimal SARIMA model on the ocean pH dataset with the original time series of the pH levels considering as test data the final 10% of the original set of values.

The selected model achieved an *AIC* of 1879.18, *BIC* of –1853.35, and residual *SE* of 0.009938, confirming a favourable trade-off between model complexity and fit performance. During the test period, the forecast maintained strong agreement with actual observations, yielding an *RMSE* of 0.0051 and *MAE* of 0.06 %. These small errors indicate that the SARIMA model can effectively represent short-term pH variability with a limited deviation from the measured values.

Minor divergence observed towards the end of 2022 remains within the 95% prediction interval and likely reflects natural short-term fluctuations or residual measurement noise rather than structural model errors. Overall, the SARIMA(1,1,1)(2,1,1)[12] configuration provides a statistically consistent and robust representation of recent marine pH behaviour, validating its use for short-term forecasting purposes.

3.2.2. SARIMA model for ocean and CO_2 series

In this particular case, the model found is represented by SARIMA(0,1,3)(0,1,1)[12], using, once again, 90% of the data to train the model and the remaining 10% for testing.

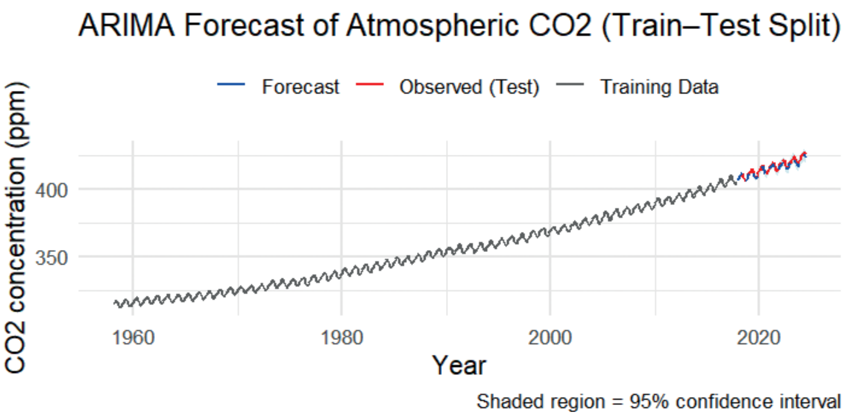

Fig. 8 - Output of the optimal SARIMA model on the ocean CO_2 dataset with the original time series of the CO_2 levels considering as test data the final 10% of the original set of values.

The SARIMA(0,1,3)(0,1,1)[12] model fitted to the monthly atmospheric CO_2 series (1958–2024) accurately represents (Fig. 8) both the persistent upward trend and the annual seasonal oscillations observed in the Mauna Loa record.

The non-seasonal differencing ($d = 1$) effectively removes the long-term linear trend associated with the progressive accumulation of atmospheric CO_2, while the seasonal differencing (D = 1) and the seasonal moving-average component (Q = 1) capture the typical annual cycle of the global carbon system. The three moving-average terms describe short-term dependencies within the residuals, indicating that recent disturbances influence subsequent CO_2 observations.

Quantitatively, the model achieved an *AIC* of 367.62, *BIC* of 390.4, and an *SE* of 0.312 ppm, confirming a parsimonious fit with low residual dispersion. The 95% confidence intervals are narrow and the forecast (blue line) closely reproduces the observed test values (red line), demonstrating strong short-term predictive performance.

As shown in Fig. 9, the model successfully reproduces the historical behaviour of the series without apparent bias, maintaining the coherence of both the seasonal pattern and the long-term increasing trend. In the validation segment (2020–2024), the predictions almost perfectly overlap the observed data, suggesting that the model is well-specified and not overfitted.

3.2.3. Short-term forecast

To evaluate the short-term forecasting capability of the model, the SARIMA(1,1,1)(2,1,1)[12] configuration was used to predict ocean pH values for the two years following the most recent observation (2023 and 2024).

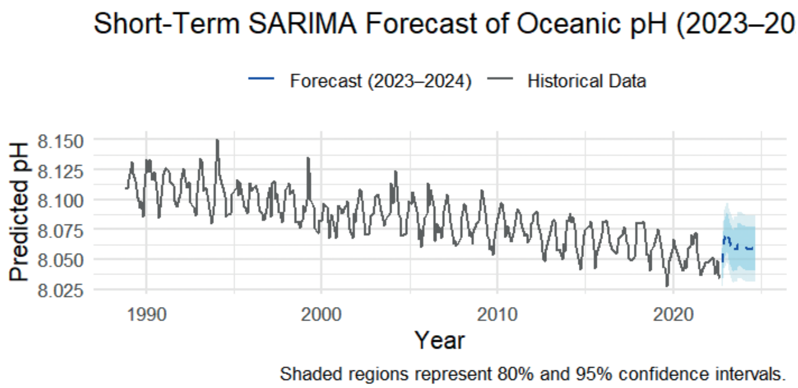

Fig. 9 – Short-term forecast of the SARIMA(1,1,1)(2,1,1)[12] and monthly frequency for the ocean pH series in terms of date, displaying the new data segment as extension of the original ocean pH dataset.

The resulting forecast, shown in Fig. 10, maintains the long-term decreasing trend with mild seasonal oscillations. The model projects a mean pH of 8.042 0.010 (95 % CI) by the end of 2024, consistent with the ongoing acidification trajectory.

As expected, the uncertainty bands widen progressively beyond the observed period, reflecting the cumulative propagation of model error. This behaviour confirms that SARIMA remains suitable for short-term forecasting (up to 24 months) but that longer extrapolations would require coupling with process-based or hybrid approaches.

The results obtained by applying the same strategy to a CO_2 model are shown in Fig. 10.

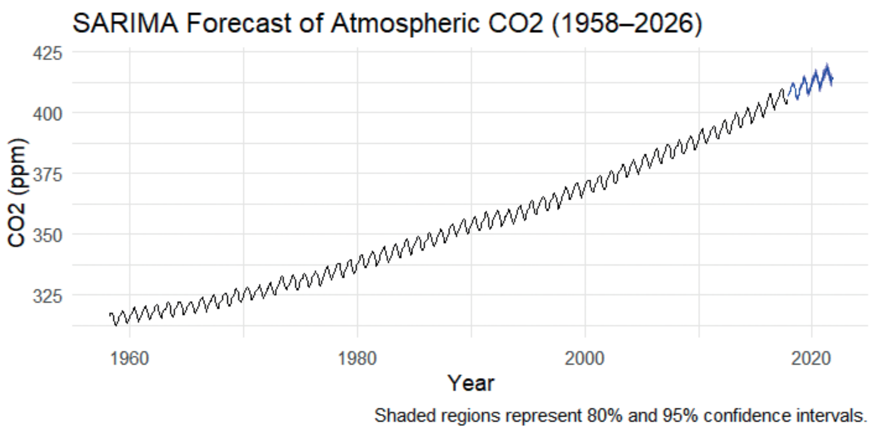

Fig. 10 - Short–term forecast of the SARIMA(0,1,3)(0,1,1)[12] and monthly frequency for the ocean pH series in terms of date, displaying the new data segment as extension of the original CO_2 dataset.

As expected, the SARIMA model was able to adjust and follow the oscillatory pattern of the CO_2 series, thus, forecasting the behaviour of atmospheric CO_2 by 2026.

3.2.4. Additional forecast estimations

By combining a robust method of regression such as STL with SARIMA models, we can extend the performance of forecasting techniques. In this case, Fig. 11 illustrates another approach to possible future values of ocean pH.

The STL + SARIMA residual model successfully reproduces the temporal behaviour of the ocean pH series from 1985 to 2022 and provides a smooth short-to-medium-term projection up to 2025. The observed historical component (blue line) shows clear interannual fluctuations with a gradual downward trend in pH, consistent with ocean acidification driven by rising atmospheric CO_2. The forecasted segment (yellow dashed line) continues this declining pattern with mild

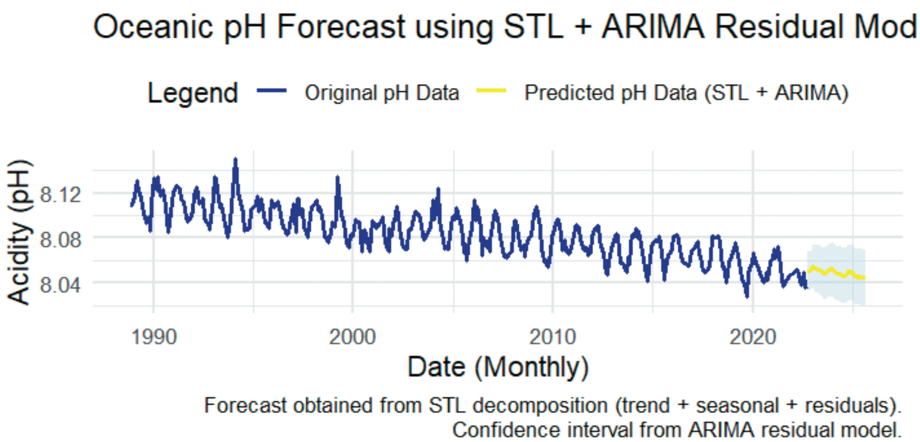

Fig. 11 -Alternative focus on forecasted values of ocean pH through SARIMA residuals combined with the STL method.

oscillations, reflecting the persistence of the long-term trend while maintaining the short-term variability inferred from the SARIMA residual structure. The shaded region represents the 95% confidence interval, which widens moderately after 2023, indicating increasing uncertainty typical of extrapolation. Despite this, the predicted pH values remain within the observed variability range of the recent years, suggesting that the STL + SARIMA hybrid model provides a stable and realistic projection of ocean acidification dynamics over the next few years.

4. Conclusions and recommendations

This study applied a sequence of statistical models to analyse and forecast the evolution of ocean pH and atmospheric CO_2 concentrations. The comparison between linear regression and autoregressive approaches demonstrated that linear methods, while simple, are insufficient to capture the nonlinear and autocorrelated nature of climate-related time series. In contrast, ARIMA-based models provided a statistically consistent representation of both the downward trend in ocean pH and the upward trajectory of atmospheric CO_2.

The optimised SARIMA (1, 1, 1)(2, 1, 1)[12] configuration achieved high short-term accuracy, maintaining low residual dispersion (SE = 0.0099) and tight confidence intervals during out-of-sample validation. Similarly, the CO_2 SARIMA (0, 1, 3)(0, 1, 1)[12] model effectively reproduced both long-term growth and annual oscillations, confirming the reliability of autoregressive modelling for short-range prediction.

However, due to the cumulative propagation of forecast uncertainty, the SARIMA framework becomes less stable for medium- and long-term horizons. To address this limitation, a hybrid STL + SARIMA approach, decomposing the pH series into trend, seasonal, and residual components, was implemented. This hybridisation enhanced forecast smoothness and consistency up to 2025, while preserving the seasonal signal and overall declining pattern. The results indicate that STL +

SARIMA can mitigate error amplification typical of pure autoregressive models, offering a more robust alternative for medium-term projections of ocean acidification.

Future work should explore multivariate and machine learning hybridisations, e.g. SARIMA combined with back-propagation neural networks or support vector regression to extend predictive capability while maintaining interpretability. In parallel, integrating physical or chemical constraints from ocean-carbon models could improve the extrapolation of pH beyond short-term horizons.

Overall, the findings confirm that statistical modelling, particularly when extended through hybrid methods like STL + SARIMA, constitutes a viable and transparent framework for forecasting environmental indicators (such as ocean pH) complementing process-based simulations, and supporting climate-change monitoring.

Acknowledgments. The author would like to express his sincere appreciation to Issys Z. Cano for her support and assistance in enhancing the quality of this paper through a complete review of each section and statement. Every R script created to generate the results, data extraction, and manipulation and optimisation procedures can be found at https://doi.org/10.5281/zenodo.13924425. The most current CO_2 emission database is publicly provided by NASA, while the ocean pH dataset is displayed by the Copernicus Marine Team (Copernicus Marine Service, 2022). However, should both datasets be under review, they can be found as CSV files at https://doi.org/10.5281/zenodo.13924425.

REFERENCES

Box G.E.P. and Jenkins G.M.; 1970: *Time series analysis: forecasting and control, 1st ed.* Holden-Day series in time series analysis, University of Minnesota, ISBN: 0816210942, 9780816210947.

Box G.E.P., Jenkins G.M., Reinsel G.C. and Ljung G.M., 2016: *Time series analysis: forecasting and control*, *5th ed.* John Wiley and Sons Inc., Hoboken, NJ, USA, pp. 712, ISBN: 978-1-118-67502-1, doi: 10.1111/jtsa.12194.

Caldeira K. and Wickett M.E.; 2005: *Ocean model predictions of chemistry changes from carbon dioxide emissions to the atmosphere and ocean.* J. Geophys. Res.: Atmospheres, 110, C09S04, doi: 10.1029/2004JC002671.

Cleveland R.B., Cleveland W.S., McRae J.E. and Terpenning I.; 1990: *STL: a Seasonal-trend decomposition procedure based on Loess*. Journal of Official Statistics, 6, 3–73, https://tinyurl.com/4wvyryrd.

Copernicus Marine Service; 2022: *Global Ocean acidification - mean sea water pH time series and trend from multi-observations reprocessing*. https://marine.copernicus.eu/access-data/ocean-monitoring-indicators/global-ocean-acidification-mean-sea-water-ph-time-series**.**

De Livera A.M., Hyndman R.J. and Snyder R.D.; 2011: *Forecasting time series with complex seasonal patterns using exponential smoothing*. Journal of the American Statistical Association, 106(496), 1513–1527,doi: 10.1198/ jasa.2011.tm09771.

Dodge Y.; 2008: *Least absolute deviation regression*. In: The Concise Encyclopedia of Statistics, Springer Science, Business Media, New York, NY, USA, pp. 502-505, ISBN: 978-0-387-32833-1.

Doney S., Fabry V., Feely R. and Kleypas J.; 2009: *Ocean acidification: the other CO2 problem*. Ann. Rev. Mar. Sci., 1, 169-92, doi: 10.1146/annurev.marine.010908.163834.

EEA (European Environment Agency); 2024: *Ocean acidification.* https://www.eea.europa.eu/en/analysis/indicators/ocean-acidification.

Hyndman R. and Khandakar Y.; 2008: *Automatic time series forecasting: the forecast package for R*. J. Stat. Softw., 27, doi: 10.18637/jss.v027.i03.

Hyndman R.J. and Athanasopoulos G.; 2021: *Forecasting: principles and practice (3rd ed.).* OTexts, https://otexts.com/fpp3/.

Kang Y., Hyndman R.J. and Smith-Miles K.; 2017: *Visualising forecasting algorithm performance using time series instance spaces.* International Journal of Forecasting, 33(2), 345–358, doi: 10.1016/j.ijforecast.2016.09.004.

Keeling C.D., Bacastow R.B., Bainbridge A.E., Ekdahl C.A., Guenther P.R., Waterman L.S. and Chin J.F.S.; 1976: *Atmospheric carbon dioxide variations at Mauna Loa Observatory, Hawaii.* Tellus, 28(6), doi: 10.3402/tellusa.v28i6.11322.

NOAA (National Oceanic and Atmospheric Administration); 2024: *Carbon Dioxide.* https://research.noaa.gov/category/climate/carbon-dioxide/.

NOAA (National Oceanic and Atmospheric Administration); 2025: *Ocean acidification.* https://www.noaa.gov/education/resourcecollections/ocean-coasts/ocean-acidification.

Rockström J., Steffen W., Noone K., Persson Å., Chapin III F.S., Lambin E., Lenton T.M., Scheffer M., Folke C., Schellnhuber H., Nykvist B., De Wit C.A., Hughes T., van der Leeuw S., Rodhe H., Sörlin S., Snyder P.K., Costanza R., Svedin U., Falkenmark M., Karlberg L., Corell R.W., Fabry V.J., Hansen J., Walker B., Liverman D., Richardson K., Crutzen P. and Foley J.; 2009: *Planetary boundaries: exploring the safe operating space for humanity.* Ecology and Society, 14(2), 32, https://ecologyandsociety.org/vol14/iss2/art32/.

Schmidt P., Kwiatkowski D., Phillips P.C.B. and Shin Y.; 1992: *Testing the null hypothesis of stationarity against the alternative of a unit root: how sure are we that economic time series have a unit root?* Journal of Econometrics. 54 (1–3): 159–178. doi:10.1016/0304-4076(92)90104-Y.

Sutton A.J., Battisti R., Carter B., Evans W., Newton J., Alin S., Bates N.R., Cai W.-J., Currie K., Feely R.A., Sabine C., Tanhua T., Tilbrook B. and Wanninkhof R.; 2022: *Advancing best practices for assessing trends of ocean acidification time series*. Frontiers in Marine Science, 9, https://doi.org/10.3389/fmars.2022.1045667.

Villavicencio J.; 2018: *Introducción a Series de Tiempo.* 31 pp., https://www.studocu.com/pe/document/universidad-nacional-agraria-la-molina/economia/introduccion-a-series-de-tiempo/88949854.

Zeebe R.E., Zachos J.C., Caldeira K. and Tyrrell T.; 2008: *Carbon emissions and acidification*. Science, 321, 51-52, doi: 10.1126/science.11591.

Corresponding author: Nelson Lucio Rodríguez
Villa del Rosario, Norte de Santander
Colombia
Phone: +57 3202737760; e-mail: elitedead17@gmail.com